# Methodological CASPT2 study of the valence excited states of an iron-porphyrin complex

Nadia Ben Amor, Adrien Soupart, Marie-Catherine Heitz

Journal of Molecular Modeling

# Valence excited states of metalloporphyrins studied with the CASPT2 method: the case of an Iron complex

--Manuscript Draft--

| | |
|---|---|
| **Manuscript Number:** | |
| **Full Title:** | Valence excited states of metalloporphyrins studied with the CASPT2 method: the case of an Iron complex |
| **Article Type:** | TC Festschrift H. Chermette |
| **Keywords:** | Iron-porphyrins; CASSCF; MS-CASPT2; IPEA shift |
| **Corresponding Author:** | Nadia Ben Amor<br>CNRS / Université Paul Sabatier<br>Toulouse, FRANCE |
| **Corresponding Author Secondary Information:** | |
| **Corresponding Author's Institution:** | CNRS / Université Paul Sabatier |
| **Corresponding Author's Secondary Institution:** | |
| **First Author:** | Nadia Ben Amor |
| **First Author Secondary Information:** | |
| **Order of Authors:** | Nadia Ben Amor |
| | Adrien Soupart |
| | Marie-Catherine Heitz |
| **Order of Authors Secondary Information:** | |
| **Abstract:** | The singlet valence excited states of an iron-porphyrin-pyrazine-carbonyl complex are investigated up to the Soret band (about 3.eV) using Multi-State Complete Active Space with Perturbation at the Second Order (MS-CASPT2). This complex is a model for the active site of carboxy-hemoglobin/myoglobin. The spectrum of the excited states is rather dense, comprising states of different nature: d→pi* transitions, d→d states, pi→pi* excitations of the porphyrin and doubly excited states involving simultaneous intra-porphyrin pi→pi* and d→d transitions. Specific features of the MS-CASPT2 method are investigated. The effect of varying the number of roots in the state average calculation is quantified as well as the consequence of targeted modifications of the active space. The effect of inclusion of standard Ionization Potential-Electron Affinity (IPEA) shift in the perturbation treatment is also investigated. |

# Valence excited states of metalloporphyrins studied with the CASPT2 method: the case of an Iron complex

*Nadia Ben Amor*, Adrien Soupart, Marie-Catherine Heitz**

Laboratoire de Chimie et Physique Quantiques UMR5626, IRSAMC, CNRS/Université Paul Sabatier 118 Rte de Narbonne 31 062 Toulouse Cedex France

Corresponding authors: heitz@irsamc.ups-tlse.fr, benamor@irsamc.ups-tlse.fr

The singlet valence excited states of an iron-porphyrin-pyrazine-carbonyl complex are investigated up to the Soret band (about 3.eV) using Multi-State Complete Active Space with Perturbation at the Second Order (MS-CASPT2). This complex is a model for the active site of carboxy-hemoglobin/myoglobin. The spectrum of the excited states is rather dense, comprising states of different nature: d→π* transitions, d→d states, π→π* excitations of the porphyrin and doubly excited states involving simultaneous intra-porphyrin π→π* and d→d transitions. Specific features of the MS-CASPT2 method are investigated. The effect of varying the number of roots in the state average calculation is quantified as well as the consequence of targeted modifications of the active space. The effect of inclusion of standard Ionization Potential-Electron Affinity (IPEA) shift in the perturbation treatment is also investigated.

**Keywords**

Iron-porphyrins, CASSCF, MS-CASPT2, IPEA shift

## Introduction

Heme proteins are responsible for many biological functions like transport, storage and detection of ligands and catalytic activities. For example, hemoglobin and myoglobin are well known for assuming the transport and the storage of the $O_2$ molecule. But their active centers can also interact with other diatomics, in particular with the CO poisoning molecule which can strongly bind to iron porphyrin sites. Advantage of the IR-spectroscopic response of CO can be taken to perform vibrational ladder climbing[1] and to probe the ligand dissociation and transfer inside the protein[2–4]. Photodissociation of the iron-CO bond following excitation with visible or near UV light has been reported experimentally[5, 6] and theoretically investigated with TD-DFT[7–9]. However, further investigations are needed to get a deeper insight of the nature of the excited states involved in the dissociation process and, as a perspective, in the accompanying spin relaxation process from S=0 to S=2 (unligated active site). In this paper, we present Multi-State Complete Active Space with Perturbation at the Second Order[10] (MS-CASPT2) calculations of the valence singlet excited states (< 3.5eV) of a model of the active site of carboxyhemoglobin or carboxymyoglobin. The model complex consists of an iron center in a porphyrin (P), with CO and pyrazine (pz) as axial ligands (FeP(pz)CO).

In the 1960s, Gouterman proposed a four orbitals model to rationalize the absorption spectra of porphyrins in terms of combinations of one-electron transitions between frontier π orbitals of the macrocycle[11, 12]. Since this early work, interest for a theoretical description of porphyrin-based systems has not decreased, taken advantage of the development of ab initio methods for the treatment of electronic excited states[13–22].

Iron-porphyrin complexes belong to the class of so-called irregular porphyrins where the partially filled d-shell contributes significantly to the excited state spectrum by introducing excitations from/to metallic orbitals. Particular attention must thus be given to the description of the interaction of the metal and the ligand(s), porphyrin ligand and axial ligand(s) if present. A recent overview on multiconfiguration ab initio methods applied on heme-related systems, summarizing ground and low-lying states calculations, can be found in Reference [23]. CASPT2 determination of spin-state energetics[24, 25] and of binding energies of small molecules on heme[26] have been reported and in some cases used to assess the validity of

various density functionals. Particular interest is shown for the addition reaction of $O_2$ to heme[27, 28] and for the characterization of the iron-$O_2$ bond[29, 30]. Relative energies of spin-states of manganese complexes involving either a porphyrin ligand[31] or related corrole or corrolazine ligands[32] are also reported in the literature. In all these CASPT2 calculations, the active space includes pure metallic and metal-ligand bonding/antibonding orbitals and possibly axial ligand orbitals. Massive inclusion of $\pi$ and $\pi^*$ orbitals of the porphyrin ring is not possible in a Complete Active Space Self Consistent Field[33] (CASSCF) active space. A possible approach consists in a set-up of the active space in order to take into account only the most important orbitals, at least those for which the occupation numbers vary significantly. Another solution consists in performing a Restricted Active Space Self Consistent Field (RASSCF)[33] scheme, which allows for considering more active orbitals while the restriction is put on the degree of excitation of the determinants. In the recent years, several studies at the RASPT2[34] level have investigated the relative energies of low-lying (mainly spin) excited states of iron, manganese, cobalt/porphyrin or corrole complexes[35–38].

In the present work, we intend to gain information on the valence excited states of the metallic center of carboxy-hemoglobin/myoglobin by means of the CASSCF/MS-CASPT2 method. The heme site is bound to the protein through the imidazole (im) group of a histidine residue. Hence, a complex restricted to the ligands directly coordinated to the iron comes down to FeP(im)CO. This standard model, used in Symmetry Adapted Cluster -CI (SAC-CI)[39, 40] and TD-DFT[7, 8] investigations of the absorption spectra of carboxyhemoglobin, has $C_s$ symmetry. Due to the high density of excited states, we choose to replace the imidazole ($C_3H_4N_2$) group by a pyrazine ($C_4H_4N_2$) group, leading to a FeP(pz)CO complex of $C_{2v}$ symmetry. We believe that the conclusions drawn from our calculations are not strongly affected by this simplification while the increase of symmetry makes the calculation more tractable. In this paper, we address the problem of the description of the singlet valence excited states of FeP(pz)CO, up to the Soret band (about 3eV). Dependence of the results on the number of roots and on modifications of the active space, as well as the behavior of the basis set with respect to the correlation of the 3s electrons of the iron, are examined. Concerning the perturbation step, the default value (0.25 a.u.) of the Ionization Potential-Electron Affinity (IPEA) shift for the zeroth order Hamiltonian[41] is controversially discussed in the literature[42–46], both for iron compounds[43, 44] and for porphyrin ones[42]. Thus, the

excited states of the iron-porphyrin complex studied here have been calculated with and without IPEA shift, and the differences analyzed.

## I. Computational details

The calculations on the iron complex have been performed at a nuclear configuration optimized at the DFT level, using the PBE0 functional[47] with the Def2QZVPP basis set[48, 49] on the iron atom and the Def2TZVP basis sets[48, 49] on the remaining atoms, employing the Gaussian 09 package[50]. The final structure, displayed in Figure 1 (plotted with MacMolPlt[51]), is a stable minimum of $C_{2v}$ symmetry, as was confirmed by a harmonic frequencies calculation. In the chosen axis system, the Fe-C-O line is the z axis and the pyrazine ligand lies in the xz plane, bisecting the two planes defined as containing opposite iron-N(porphyrin) bonds. Table 1 presents some of the interatomic distances, around the metallic center. Complete coordinates of the optimized structure can be found as Supplementary Information. A diagram of the valence orbitals of the complex with their occupations as obtained by the DFT calculation is also displayed in Figure 1 (right).

| | |
|---|---|
| Fe – C (CO) | 1.784 |
| Fe – N (pyrazine) | 2.080 |
| Fe – N (porphyrin) | 2.006 |
| C – O | 1.135 |

**Table 1:** Selected interatomic distances of the optimized structure, in Ångström.

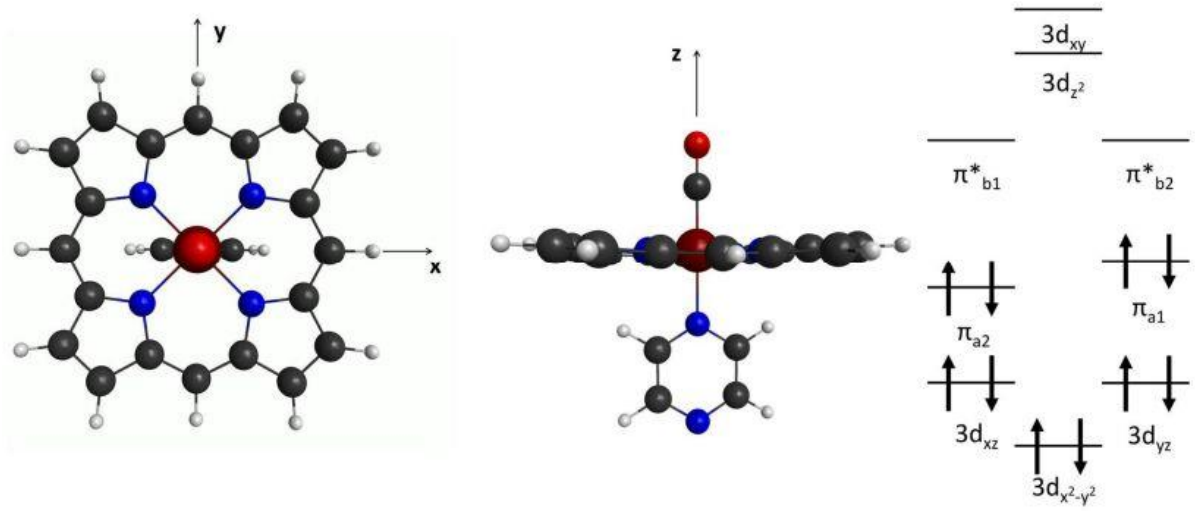


**Figure 1:** FeP(pz)CO optimized structure (see text) and occupation of the valence orbitals at the DFT level.

The calculations of the excited states were carried out with the 7.8 MOLCAS package[52–54] and were based on Relativistic Correlation Consistent Atomic Natural Orbitals (ANO-RCC)[55, 56] basis sets. Scalar relativistic effects were taken into account by using the second-order Douglas-Kroll-Hess Hamiltonian[57, 58]. For *Fe*, a (21s15p10d6f4g) basis set is contracted to [7s6p5d2f1g]; for *C, N, O* a (14s9p4d) set is contracted to [4s3p1d] and for *H* a (8s4p) set is contracted to [2s1p]. The ANO-RCC basis set for the iron atom has been developed without correlating the 3s electrons, *i.e.*, these electrons are described with minimal basis quality[56]. It is mentioned in the original publication that these electrons *should not be included in any correlation treatment, because that could cause large basis set superposition errors*[56]. However, in most of the iron studies using ANO-RCC basis sets, the 3s electrons are correlated. Thus, an additional test calculation has been performed to check the validity of correlating the 3s electrons, using another relativistic all-electron correlation consistent basis set for the iron atom, the aug-cc-pwCVTZ-DK [9s8p6d3f2g][59], which takes into account the semi-core correlation of the [3s,3p] electrons, while the ligands are still described by the ANO-RCC basis set.

Concerning the active space, a straightforward inclusion of all valence π and π* orbitals of the porphyrin and of all orbitals with significant 3d metallic contribution would result in a 36 electrons in 36 orbitals active space which exceeds by far the current computational possibilities of the CASSCF method. Compromises have thus to be done. Our

smallest active space includes the 3d orbitals of Fe, the 3d' double shell orbitals correlating the three (ground state) occupied 3d orbitals of Fe and the two metal-ligand σ-bonding orbitals counterpart of the empty 3d iron orbitals, supplemented by four orbitals of the porphyrin ring. These latter are the so-called Gouterman's orbitals which consist in the four frontier orbitals of the porphyrin ring (two occupied and two unoccupied). This leads to 14 electrons in 14 orbitals, noted CAS(14,14). Figure 2 presents a sketch of the active orbitals (plotted with Molekel[60]). Note that the π* orbitals of the porphyrin ring have a metallic contribution and that the $3d'_{xz}$ and $3d'_{yz}$ orbitals are mixed with the π* orbitals of CO. Such an active space is intended to include all the orbitals whose occupation varies significantly between the ground and the excited states, for states below the Soret band (the second set of intraporphyrin π→π* transitions) and fulfill the basic recommendations for first row transition metal compounds. The situation is more complicated for the Soret band. Even if excitations among the Gouterman's set are still dominant, the results of SAC-CI studies [39, 40] point out excitations from the two next occupied π orbitals of the macrocycle. On this basis, attempts have been made to include the second highest occupied porphyrin π orbitals (one of $A_1$, the other of $A_2$ symmetry) in the active space leading to a cumbersome but still tractable 18 electrons in 16 orbitals calculation, but it was never possible to stabilize the targeted $a_1$ orbital in the active space.

Three other active spaces resulting from the inclusion of two unoccupied orbitals have been tested. A-CAS(14,16) includes the two remaining 3d' orbitals which correlate the 3d orbitals at most singly occupied in all the states considered. B-CAS(14,16) includes the two π* orbitals of CO while C-CAS(14,16) includes two unoccupied π* orbitals of the porphyrin ring, of $A_1$ and $A_2$ symmetry respectively (see Supplementary Information for the representation of these latter orbitals). We intend to investigate the excited states of the FeP(pz)CO complex up to the Soret band. Ten roots at the CASSCF level are thus calculated for each symmetry. State specific orbitals are sometimes impossible to obtain and average orbitals are generally a good compromise to get the whole set of states involved in the electronic spectrum. In order to estimate the effect of using state-average orbitals, we perform also, in addition to the ten roots MS-CASPT2, three or four roots state-average calculations for selected cases. Vertical excitations energies were always calculated considering the

ground and excited states at the same level of calculation (same number of roots, same active space).

In all cases, Cholesky decomposition technique[61, 62] which allows a drastic reduction of the number of bielectronic integrals, is used, with a $10^{-6}$ a.u. threshold. To avoid intruder states, a level shift of 0.4 a.u. has been used in all the MS-CASPT2 calculations, which is the lowest common value that gives similar reference weights for all states.

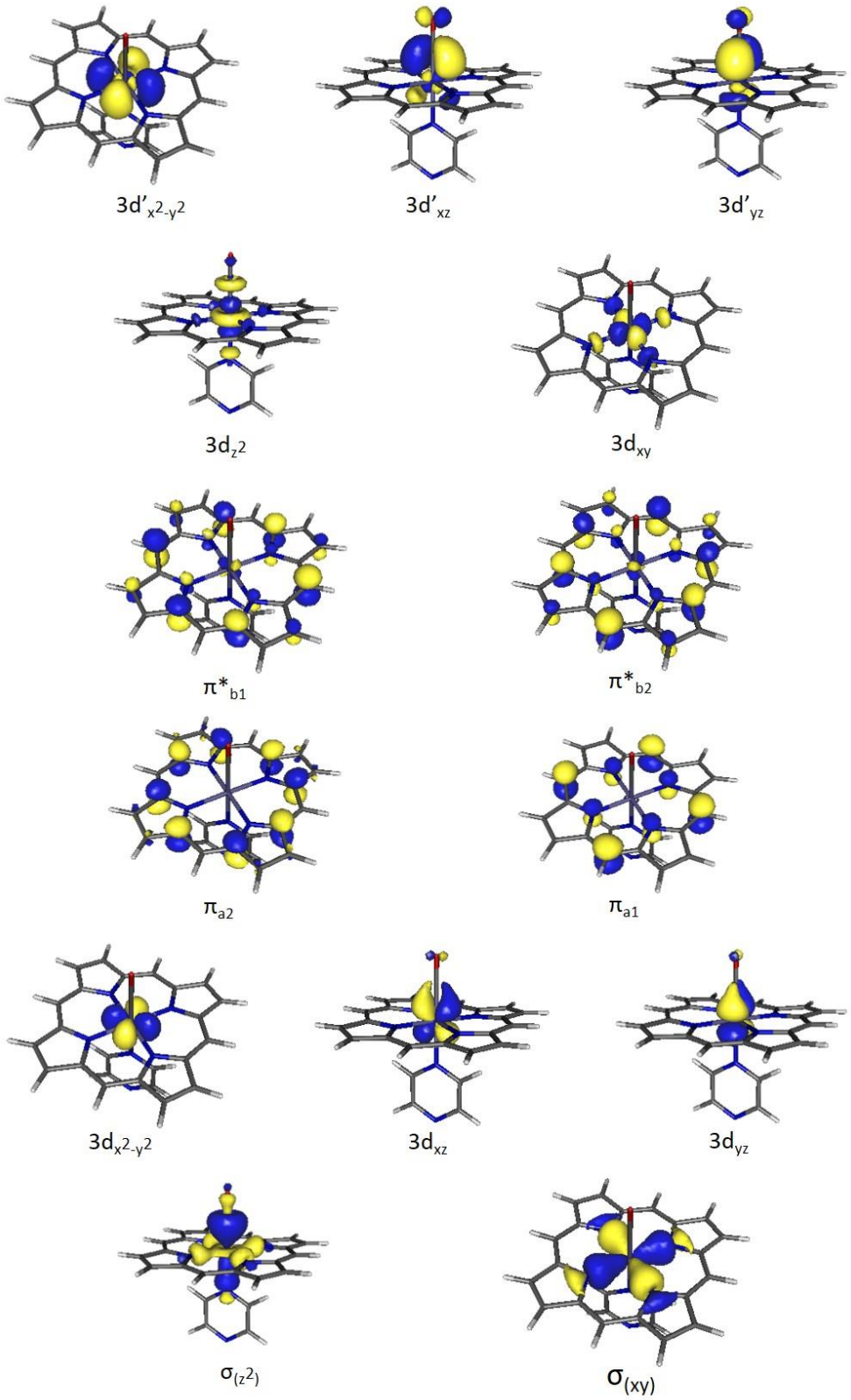


**Figure 2:** Active orbitals from a 10-roots state average CASSCF (CAS(14,14)) of $A_1$ symmetry.

## II. Results and Discussion

### 1. Correlation of the 3s electrons

In CASPT2 calculations, core electrons, like the 1s, 2s, 2p electrons of Fe and the 1s electrons of C,N and O, are usually frozen. As mentioned in the computational details, the ANO-RCC basis set of the iron atom has been set up without including the correlation of the 3s electrons[56]. As these electrons are often correlated, a test calculation has been performed on the first $A_1$ excited states of the compound. In Table 2, we present excitation energies for two basis sets, in the case of either frozen or correlated 3s electrons. For the aug-cc-pwCVTZ-DK basis sets, which takes into account the semi-core correlation of the [3s,3p] electrons and not only the [3p], the two sets of excitation energies differ from at most 0.12 eV. This is small but not negligible, therefore the 3s electrons should be correlated, as expected. As the transition energies between the two basis sets differ from at most 0.01 eV, for frozen and for correlated 3s electrons, we can conclude that, when the ANO-RCC basis is used for iron, the correlation of the 3s electrons does not cause basis set superposition errors in this molecular system. In all the rest of the study, these electrons are thus included in the correlation calculations.

| | ANO-RCC [7s6p5d2f1g] | | aug-cc-pwCVTZ [9s8p6d3f2g] | |
|---|---|---|---|---|
| | 3s correlated | 3s frozen | 3s correlated | 3s frozen |
| | ΔE (eV) | ΔE (eV) | ΔE (eV) | ΔE (eV) |
| $d \rightarrow \pi^*$ | 1.64 | 1.68 | 1.64 | 1.68 |
| $d \rightarrow \pi^*$ | 1.93 | 1.96 | 1.93 | 1.96 |
| $d \rightarrow d$ | 2.90 | 3.02 | 2.89 | 3.01 |

**Table 2:** Effect of the correlation of the 3s electrons of the iron on the excitation energies of the first $A_1$ excited states of the FeP(pz)CO molecule (eV), for different basis sets on the iron and different frozen orbital schemes. MS-CASPT2 on 4-roots CAS(14,14) (see text) and IPEA=0.0 a.u.

## 2. State average orbitals

The results discussed in this subsection are all obtained without inclusion of the IPEA shift. As state specific evaluation of all the states of interest is often problematic, state average (SA) orbitals –which provide most of the time a well-balanced description of the different states- are used. The number of states for which density matrices are averaged can have a quite important effect on the total energies. The goal is here to analyze the effect on the transition energies. We intend to calculate the states up to the Soret band (about 3. eV), which corresponds to the second set of $\pi \rightarrow \pi^*$ excitations. At the CASSCF(14,14) level, these states correspond to the 8th roots of $B_1$ and $B_2$ symmetries while in the different CAS(14,16) active spaces these states correspond either to the $8^{th}$, $9^{th}$ or $10^{th}$ root. Hence, we calculate the excited states on the basis of 10-roots SA-CASSCF/MS-CASPT2. In the $A_1$ and $A_2$ symmetries, where a fewer number of mono-excitations are involved, it is possible to obtain the lowest valence states by averaging over a smaller number of states. Table 3 displays excitation energies of the electronic states dominated by mono-excitations of $A_1$ symmetry, at the MS-CASPT2 level, based on a SA-CASSCF involving either 10, 4 or 3 roots. The fourteen active orbitals issued from the 3- and 4-roots calculations have very similar shapes as compared to those displayed in Figure 2 (issued from a 10-roots average), except for the occupied $\pi$ orbital of $A_1$ symmetry which has a significant contribution of iron-carbonyl $\sigma$-bonding type. The 4-roots calculation results in three excited states of clearly identified characters, two Metal to Ligand Charge Transfer (MLCT) states and a ligand field transition to the $d_z^2$ orbital (Metal Centered –MC- states). The two groups of states are rather well separated in energy and when additional roots are included in the CASSCF procedure, mainly doubly excited states supplement the set. These doubly excited states can be described as two mono-excitations localized on two subsystems, namely a $d \rightarrow d$ transition and an intra-porphyrin $\pi \rightarrow \pi^*$ transition. After the MS-CASPT2 step, two such states are found below the ligand field excitation. This type of states will be discussed in the next subsection. Including more roots in the calculation has a greater effect on the MLCT excitation energies than on the $d \rightarrow d$ transition. This can be explained by considering the varying oxidation numbers of the iron in the different states. In the MLCT states, the iron has mainly a $d^5$ configuration while all other states are $d^6$. So the 10-roots averaged CASSCF orbitals might be less adapted to the description of the MLCT states than those of the 4-roots calculation where $d^5$ and $d^6$

configurations have balanced weights. Also included in the same table are the results of a three roots calculation, in principle slightly biased in favor of $d^5$ states, which are similar to those of the four roots calculation. A comparison of 10-roots and 3-roots transition energies for the MLCT states shows difference of as much as 0.3-0.35 eV. However, the effect of varying the number of roots is different for the $A_2$ symmetry (Table 4). There, a 3-roots calculation (again two MLCT and one MC states) is compared to a 10-roots calculation. The three states are close in energy in both calculations but the nature of the states changes. In the three roots calculation, MCLT and MC characters are mixed for two of the states. Hence, the assignment of the states is changed but the excitation energies vary at most of 0.16 eV (0.1 eV for the pure MLCT state).

| **$A_1$** | **10-roots** | | **4-roots** | | **3-roots** | |
|---|---|---|---|---|---|---|
| Ground state $(d_{x2-y2})^2(d_{xz})^2(d_{yz})^2(\pi_{a2})^2(\pi_{a1})^2$ | Energy (a.u.) | Weight | Energy (a.u.) | Weight | Energy (a.u.) | Weight |
| | -2635.374664 | 0.81 | -2635.369656 | 0.81 | -2635.368812 | 0.80 |
| Excited states | **ΔE (eV)** | Weight | **ΔE (eV)** | Weight | **ΔE (eV)** | Weight |
| $d_{yz} \rightarrow \pi^*_{b2}$ | 1.39 | 0.40 | 1.64 | 0.38 | 1.76 | 0.39 |
| $d_{xz} \rightarrow \pi^*_{b1}$ | | 0.30 | | 0.41 | | 0.44 |
| $d_{yz} \rightarrow \pi^*_{b2}$ | 1.72 | 0.25 | 1.93 | 0.40 | 2.01 | 0.42 |
| $d_{xz} \rightarrow \pi^*_{b1}$ | | 0.36 | | 0.36 | | 0.37 |
| $d_{x2-y2} \rightarrow d_{z2}$ | 2.79 | 0.68 | 2.90 | 0.74 | | |

**Table 3: State average orbitals**. Excitation energies of $A_1$ symmetry states from MS-CASPT2 based on SA-CASSCF(14,14) performed with different number of roots. The value of the IPEA shift is 0. a.u.. Configurations with a weight larger than 10% are listed.

| **$A_2$** | **10-roots** | | **3-roots** | |
|---|---|---|---|---|
| State | **ΔE (eV)** | Weight | **ΔE (eV)** | Weight |
| $d_{yz} \rightarrow \pi^*_{b1}$ | 1.86 | 0.14 | 1.89 | 0.25 |
| $d_{xz} \rightarrow \pi^*_{b2}$ | | **0.54** | | < 0.01 |
| $d_{x2-y2} \rightarrow d_{xy}$ | | 0.05 | | **0.58** |
| $d_{yz} \rightarrow \pi^*_{b1}$ | 1.89 | **0.56** | 1.96 | 0.12 |
| $d_{xz} \rightarrow \pi^*_{b2}$ | | 0.13 | | **0.69** |
| $d_{x2-y2} \rightarrow d_{xy}$ | | < 0.01 | | 0.02 |
| $d_{yz} \rightarrow \pi^*_{b1}$ | 2.05 | < 0.01 | 1.98 | **0.47** |
| $d_{xz} \rightarrow \pi^*_{b2}$ | | 0.04 | | 0.14 |
| $d_{x2-y2} \rightarrow d_{xy}$ | | **0.76** | | 0.22 |

**Table 4: State average orbitals**. Excitation energies of $A_2$ symmetry states from MS-CASPT2 based on state average CAS(14,14) performed with different number of roots. The value of the IPEA shift is 0. a.u..

Such a study is not possible for the $B_1$ symmetry where there is only one d→π* configuration and where two doubly excited states are energetically in between the five mono-excitations at the CASSCF level. In $B_1$, calculations with 7, 8 and 10 roots give very close results (between 0.01 and 0.04 eV of deviation) at the MS-CASPT2 level.

### 3. Inclusion of the IPEA shift

In the CASPT2 method, the zeroth-order Hamiltonian is based on Fock-type one-electron operators. It means that the two-electron terms are not taken into account in the Hamiltonian. A systematic error is then present in the original formulation of the CASPT2 method and open-shell configurations are favored compared to closed-shell one. Several corrections have been developed such as the G1, G2 and G3[63] or the IPEA shift[41]. The IPEA shift modifies the zeroth order Hamiltonian[41] to correct this systematic error, using a single parameter whose value has been selected from benchmark calculations. But, the default value (0.25 a.u.) of this shift is regularly disputed[42–46]. Tables 5 and 6 present a comparison of the transition energies calculated at the MS-CASPT2 level based on a 10-roots SA CASSCF with and without the inclusion of the IPEA shift of 0.25 a.u. (standard value), for the $A_1$ and $B_1$ symmetries respectively. The corresponding tables for the $B_2$ and $A_2$ symmetries are enclosed as supplementary material. The states of transition energies below 3.3 eV (value

without IPEA) are reported in the tables. The spectrum of the excited states is rather dense, comprising states of different nature. There are six d→π* states, six d→d states, four π→π* states and fifteen doubly excited states, four of these latter having a porphyrin to metal charge transfer additional contribution. It is found that the effect on the excitation energies of inclusion of IPEA can be very large and is correlated to the type of excitation. Standard IPEA increases excitation energies of d→d states of an amount ranging from 0.11 to 0.45 eV. Excitation energies of MLCT states increase of about 0.5-0.9 eV while states dominated by π→π* excitations between porphyrin frontier orbitals are shifted up from about 1 eV. The effect on doubly excited states is even larger, between 0.9 and 1.4 eV. As a consequence, the energetic order of the states is markedly altered. For instance, in $A_1$ symmetry, the d→d transition is now lower than the doubly excited states and in $B_1$ the relative order of the d→d and π→π* transitions is reversed. This last remark holds also for the states of $B_2$ symmetry which are very similar to those of $B_1$. In the $A_2$ symmetry, the lowest excited state is now a d→d transition instead of a MLCT state. In Figure 3, we present a graph of the excitation energies of the states of all symmetries with IPEA shifts of 0., 0.1, 0.2 and 0.25 a.u, with a color code corresponding to the nature of the electronic excitation. The effect is clearly differentiated according the type of excitation. The blue curves corresponding to d→d transitions cross the other curves which are more or less parallel. The most striking effect when introducing IPEA is the change of relative position of d→d and π→π* states.

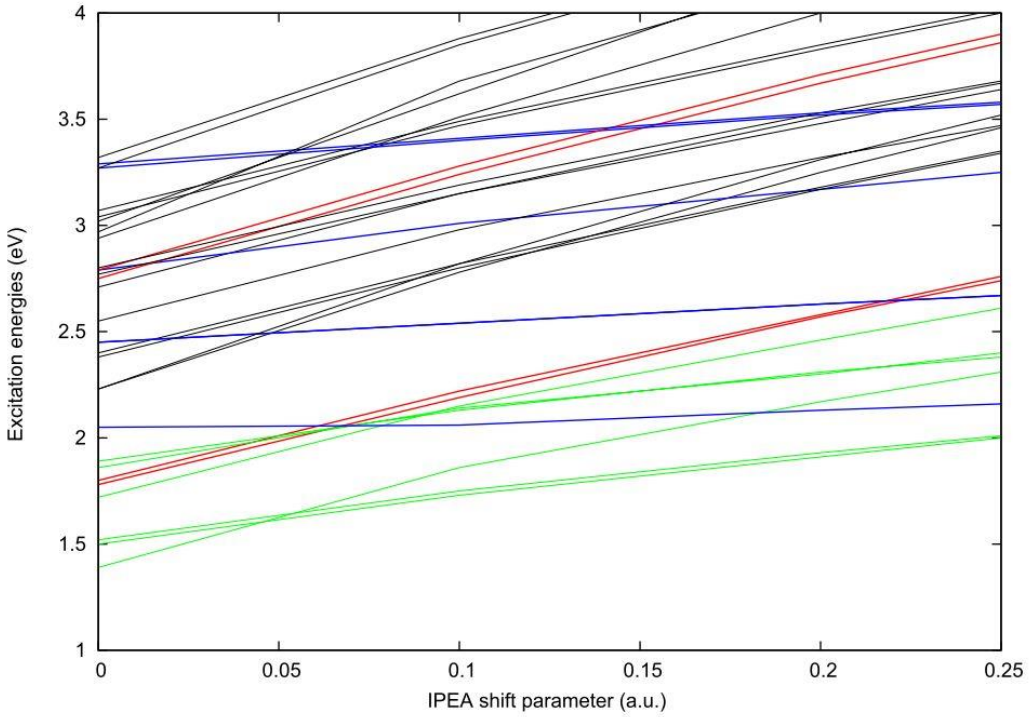


**Figure 3: Effect of IPEA**. Excitations energies of the states of $A_1$,$B_1$,$B_2$ and $A_2$ symmetries for different values of IPEA shift (0., 0.1, 0.2 and 0.25 a.u.) classified according to the nature of dominant electronic configurations: d→d (blue), π→π* (red), d→π* (green) and doubly excited states (black).

In the original publication introducing IPEA[41], excitation energies of $N_2$ and benzene molecules are reported for IPEA shifts varying from 0.0 to 0.5 a.u. In these examples, a value of IPEA of 0.25 a.u. increases the excitation energies from about 0.2 to 0.4 eV[41]. This is in the order of magnitude of the shifts observed for the d→d transitions of the iron porphyrin complex, while the MLCT and intra-porphyrin states are more destabilized. As mentioned above, the effect is even larger for some doubly excited states. No experimental results are available for FeP(pz)CO in the gas phase, but the experimental absorption spectrum of carboxyhemoglobin, for which the minimal description of the active site consists in a FeP(im)CO complex, is available in the literature[64]. The lowest absorption bands (the Q band at 2.18 and 2.30 eV and the strong Soret band at 2.96 eV[64]) are usually assigned to intra porphyrin π→π* transitions mainly due to excitation amongst the four Gouterman frontiers orbitals[8, 39]. The π→π* states are of $B_1$ and $B_2$ symmetry. As can be seen in Table 6, the value of the second π→π* transition (2.75 eV) without IPEA shift is in much better agreement with the experimental Soret band maximum than the value with standard

IPEA (3.86 eV). But for the first π→π* transition, the experimental value lies in between the results with and without IPEA (2.74 and 1.78 eV respectively). Note that excitation energies of $B_2$ symmetry states are very close to those of $B_1$. The splitting of the Q band reported experimentally is thus probably due to the environmental effect of the protein which namely tilts slightly the Fe-CO bond with respect to the porphyrin plane normal. Due to the very large effect observed for most of the transitions, between the inclusion of standard IPEA (0.25 a.u) and its omission, it seems reasonable to choose, for this particular system, the omission. CASPT2 is not intended to turn into a parametrical method. However, we mention that setting the IPEA value at 0.1 a.u. would result in the first π→π* transitions to be at 2.19 and 2.22 eV and the second ones to be at 3.24 and 3.28 eV, in reasonable agreement with the closest available experimental data, and with TD-DFT on FeP(im)CO[8].

Recent RASPT2 study compares excitation energies with no IPEA shift and with IPEA = 0.25 a.u. for FBP, MgP and ZnP[42] and concludes that the calculations without IPEA shift are in better agreement with experiments and reports that the discrepancy is more pronounced when the active space is truncated.

| $A_1$ | No IPEA | | Standard IPEA (0.25 a.u.) | | |
|---|---|---|---|---|---|
| State | ΔE (eV) | Weight | | ΔE (eV) | Weight |
| ground state | 0 | 0.81 | ground state | 0 | 0.83 |
| $d_{yz} \rightarrow \pi^*_{b2}$ | 1.39 | 0.40 | $d_{yz} \rightarrow \pi^*_{b2}$ | 2.31 | 0.40 |
| $d_{xz} \rightarrow \pi^*_{b1}$ | | 0.30 | $d_{xz} \rightarrow \pi^*_{b1}$ | | 0.29 |
| $d_{yz} \rightarrow \pi^*_{b2}$ | 1.72 | 0.25 | $d_{yz} \rightarrow \pi^*_{b2}$ | 2.61 | 0.29 |
| $d_{xz} \rightarrow \pi^*_{b1}$ | | 0.36 | $d_{xz} \rightarrow \pi^*_{b1}$ | | 0.40 |
| $\pi_{a1} \rightarrow d_{z2}$ | 2.23 | 0.23 | $d_{x2-y2} \rightarrow d_{z2}$ | 3.25 | 0.70 |
| $\pi_{a1}\ d_{yz} \rightarrow d_{z2}\ \pi^*_{b2}$ | | 0.21 | | | |
| $\pi_{a1}\ d_{xz} \rightarrow d_{z2}\ \pi^*_{b1}$ | | 0.20 | | | |
| $\pi_{a2} \rightarrow d_{xy}$ | 2.71 | 0.23 | $\pi_{a1} \rightarrow d_{z2}$ | 3.46 | 0.24 |
| $d_{yz}\ \pi_{a2} \rightarrow \pi^*_{b2}\ d_{xy}$ | | 0.20 | $\pi_{a1}\ d_{yz} \rightarrow d_{z2}\ \pi^*_{b2}$ | | 0.23 |
| $d_{xz}\ \pi_{a2} \rightarrow \pi^*_{b1}\ d_{xy}$ | | 0.19 | $\pi_{a1}\ d_{xz} \rightarrow d_{z2}\ \pi^*_{b1}$ | | 0.22 |
| $d_{x2-y2} \rightarrow d_{z2}$ | 2.79 | 0.68 | $\pi_{a2} \rightarrow d_{xy}$ | 3.67 | 0.25 |
| | | | $d_{yz}\ \pi_{a2} \rightarrow \pi^*_{b2}\ d_{xy}$ | | 0.22 |
| | | | $d_{xz}\ \pi_{a2} \rightarrow \pi^*_{b1}\ d_{xy}$ | | 0.21 |
| $\pi_{a1}\ d_{yz} \rightarrow d_{z2}\ \pi^*_{b2}$ | 2.94 | 0.16 | $\pi_{a1}\ d_{yz} \rightarrow d_{z2}\ \pi^*_{b2}$ | 4.22 | 0.21 |
| $\pi_{a1}\ d_{xz} \rightarrow d_{z2}\ \pi^*_{b1}$ | | 0.18 | $\pi_{a1}\ d_{xz} \rightarrow d_{z2}\ \pi^*_{b1}$ | | 0.22 |
| $d_{yz}\ \pi_{a1} \rightarrow \pi^*_{b1}\ d_{xy}$ | | 0.14 | $d_{yz}\ \pi_{a1} \rightarrow \pi^*_{b1}\ d_{xy}$ | | 0.15 |
| $d_{xz}\ \pi_{a1} \rightarrow \pi^*_{b2}\ d_{xy}$ | | 0.09 | $d_{xz}\ \pi_{a1} \rightarrow \pi^*_{b2}\ d_{xy}$ | | 0.10 |
| $\pi_{a2}\ d_{yz} \rightarrow d_{z2}\ \pi^*_{b1}$ | 3.32 | 0.28 | $\pi_{a2}\ d_{yz} \rightarrow d_{z2}\ \pi^*_{b1}$ | 4.55 | 0.28 |
| $\pi_{a2}\ d_{xz} \rightarrow d_{z2}\ \pi^*_{b2}$ | | 0.32 | $\pi_{a2}\ d_{xz} \rightarrow d_{z2}\ \pi^*_{b2}$ | | 0.30 |

Table 5: **IPEA shift**. Excitation energies calculated at the MS-CASPT2 level based on a 10-roots SA CASSCF(14,14) without and with the inclusion of the IPEA shift of 0.25 a.u. (standard value), for the $A_1$ symmetry.

| $B_1$ | | No IPEA | | | Standard IPEA (0.25 a.u.) |
|---|---|---|---|---|---|
| State | ΔE (eV) | Weight | | ΔE (eV) | Weight |
| $d_{x2-y2} \rightarrow \pi^*_{b1}$ | 1.50 | 0.73 | $d_{x2-y2} \rightarrow \pi^*_{b1}$ | 2.00 | 0.73 |
| $\pi_{a1} \rightarrow \pi^*_{b1}$ | 1.78 | 0.54 | $d_{xz} \rightarrow d_{z2}$ | 2.67 | 0.65 |
| $\pi_{a2} \rightarrow \pi^*_{b2}$ | | 0.35 | $d_{yz} \rightarrow d_{xy}$ | | 0.21 |
| $d_{x2-y2}\ \pi_{a1} \rightarrow \pi^*_{b2}\ d_{xy}$ | 2.40 | 0.61 | $\pi_{a1} \rightarrow \pi^*_{b1}$ | 2.74 | 0.51 |
| $\pi_{a1}\ d_{x2-y2} \rightarrow \pi^*_{b2}\ d_{xy}$ | | 0.20 | $\pi_{a2} \rightarrow \pi^*_{b2}$ | | 0.38 |
| $d_{xz} \rightarrow d_{z2}$ | 2.45 | 0.66 | $d_{x2-y2}\ \pi_{a1} \rightarrow \pi^*_{b2}\ d_{xy}$ | 3.35 | 0.63 |
| $d_{yz} \rightarrow d_{xy}$ | | 0.19 | $\pi_{a1}\ d_{x2-y2} \rightarrow \pi^*_{b2}\ d_{xy}$ | | 0.21 |
| $\pi_{a1} \rightarrow \pi^*_{b1}$ | 2.75 | 0.27 | $d_{xz} \rightarrow d_{z2}$ | 3.57 | 0.19 |
| $\pi_{a2} \rightarrow \pi^*_{b2}$ | | 0.43 | $d_{yz} \rightarrow d_{xy}$ | | 0.60 |
| $d_{x2-y2}\ \pi_{a2} \rightarrow \pi^*_{b1}\ d_{xy}$ | 2.77 | 0.53 | $d_{x2-y2}\ \pi_{a2} \rightarrow \pi^*_{b1}\ d_{xy}$ | 3.64 | 0.63 |
| $\pi_{a2}\ d_{x2-y2} \rightarrow \pi^*_{b1}\ d_{xy}$ | | 0.18 | $\pi_{a2}\ d_{x2-y2} \rightarrow \pi^*_{b1}\ d_{xy}$ | | 0.21 |
| $d_{x2-y2}\ \pi_{a1} \rightarrow d_{z2}\ \pi^*_{b1}$ | 3.04 | 0.58 | $\pi_{a1} \rightarrow \pi^*_{b1}$ | 3.86 | 0.35 |
| $\pi_{a1}\ d_{x2-y2} \rightarrow d_{z2}\ \pi^*_{b1}$ | | 0.19 | $\pi_{a2} \rightarrow \pi^*_{b2}$ | | 0.47 |
| $d_{xz} \rightarrow d_{z2}$ | 3.27 | 0.17 | $d_{x2-y2}\ \pi_{a1} \rightarrow d_{z2}\ \pi^*_{b1}$ | 4.00 | 0.61 |
| $d_{yz} \rightarrow d_{xy}$ | | 0.62 | $\pi_{a1}\ d_{x2-y2} \rightarrow d_{z2}\ \pi^*_{b1}$ | | 0.20 |

Table 6: **IPEA shift**. Excitation energies calculated at the MS-CASPT2 level based on a 10-roots SA CASSCF(14,14) without and with the inclusion of the IPEA shift of 0.25 a.u. (standard value), for the $B_1$ symmetry.

The lowest doubly excited states are found energetically below some mono-excitations at the MS-CASPT2 level, whatever the value of IPEA shift. The existence of such rather low-lying doubly excited states among the valence excited states comes from the large conjugated π system of the porphyrin ligand which results in a low energy HOMO-LUMO intra-ligand gap and could be specific to partially filled d-shell metalloporphyrins. It is useful to know the energetics of such states with respect to the mono-excited states in order to assess their role in the excited states relaxation processes following excitation to the Soret band for instance. In the $B_1$ and $B_2$ symmetries, the lowest doubly excited states involve a $\pi \rightarrow \pi^*$ excitation and the $d_{x2-y2} \rightarrow d_{xy}$ excitation which correspond to the lowest MC state. Without IPEA, two such states are found at 2.40 and 2.38 eV, well below the second $\pi \rightarrow \pi^*$ states. Inclusion of standard IPEA increases the excitation energies of slightly less than 1 eV and these states are still found below the second $\pi \rightarrow \pi^*$ set. In $A_1$ and $A_2$ symmetries, the doubly excited states are not based on the lowest MC state and their occurrence at low energy cannot be justified qualitatively. Note that, in these cases, the effect of IPEA shift is larger, up to 1.4 eV.

In the present calculations, the effect of IPEA depends strongly on the nature of the leading configurations of the different states. The effect can be very large for states involving

excitation from or/and to the π system of the porphyrin, and thus an effect of the remaining π orbitals of the porphyrin cannot be excluded.

### 4. Active spaces

The CAS(14,14) active space includes all orbitals for which the occupation number varies significantly. However, some other orbitals might play a non-negligible role. Several possibilities have been considered by adding different orbitals to the CAS(14,14): i) the two missing 3d' orbitals of the iron atom, noted A-CAS(14,16) ; ii) the anti-bonding π* orbitals of the carbonyl, noted B-CAS(14,16); iii) two additional π* orbitals of the porphyrin (see supplementary material for a graphical representation) which are low lying and might affect the d→π* states, noted C-CAS(14,16). The results are presented in Table 7. Note that, unlike for the other tables, the states in the different columns are classified according to the dominant configurations and not according to increasing energies.

| **$A_1$** | **CAS(14,14)** | | **A-CAS(14,16)** | | **B-CAS(14,16)** | | **C-CAS(14,16)** | |
|---|---|---|---|---|---|---|---|---|
| | | | **3d'** | | **$\pi^*_{CO}$** | | **$\pi^*_{P}$** | |
| | **10-roots** | | **10-roots** | | **10-roots** | | **10-roots** | |
| State | **ΔE (eV)** | Weight | **ΔE (eV)** | Weight | **ΔE (eV)** | Weight | **ΔE (eV)** | Weight |
| ground state | 0 | 0.81 | 0 | 0.78 | 0 | 0.73 | 0 | 0.83 |
| $d_{yz} \rightarrow \pi^*_{b2}$ | 1.39 | 0.40 | 1.50 | 0.46 | 1.16 | 0.25 | 1.34 | 0.35 |
| $d_{xz} \rightarrow \pi^*_{b1}$ | | 0.30 | | 0.18 | | 0.45 | | 0.34 |
| $d_{yz} \rightarrow \pi^*_{b2}$ | 1.72 | 0.25 | 1.60 | 0.23 | 1.59 | 0.41 | 1.88 | 0.31 |
| $d_{xz} \rightarrow \pi^*_{b1}$ | | 0.36 | | 0.51 | | 0.19 | | 0.32 |
| $\pi_{a1} \rightarrow d_{z2}$ | 2.23 | 0.23 | 2.45 | 0.24 | 2.20 | 0.24 | 2.34 | 0.21 |
| $\pi_{a1}\, d_{yz} \rightarrow d_{z2}\, \pi^*_{b2}$ | | 0.21 | | 0.24 | | 0.23 | | 0.22 |
| $\pi_{a1}\, d_{xz} \rightarrow d_{z2}\, \pi^*_{b1}$ | | 0.20 | | 0.18 | | 0.19 | | 0.22 |
| $\pi_{a2} \rightarrow d_{xy}$ | 2.71 | 0.23 | 2.82 | 0.16 | 2.59 | 0.21 | 2.75 | 0.20 |
| $d_{yz}\, \pi_{a2} \rightarrow \pi^*_{b2}\, d_{xy}$ | | 0.20 | | 0.16 | | 0.18 | | 0.19 |
| $d_{xz}\, \pi_{a2} \rightarrow \pi^*_{b1}\, d_{xy}$ | | 0.19 | | 0.12 | | 0.16 | | 0.19 |
| $d_{x2-y2}$ -> $d_{z2}$ | | | | 0.17 | | | | 0.10 |
| $d_{x2-y2} \rightarrow d_{z2}$ | 2.79 | 0.68 | 2.89 | 0.57 | 2.72 | 0.66 | 2.92 | 0.61 |
| $\pi_{a1}\, d_{yz} \rightarrow d_{z2}\, \pi^*_{b2}$ | 2.94 | 0.16 | 3.04 | 0.16 | 2.98 | 0.19 | 3.09 | 0.21 |
| $\pi_{a1}\, d_{xz} \rightarrow d_{z2}\, \pi^*_{b1}$ | | 0.18 | | 0.19 | | 0.21 | | 0.20 |
| $d_{yz}\, \pi_{a1} \rightarrow \pi^*_{b1}\, d_{xy}$ | | 0.14 | | 0.13 | | 0.14 | | 0.12 |
| $\pi_{a2}\, d_{yz} \rightarrow d_{z2}\, \pi^*_{b1}$ | 3.32 | 0.28 | 3.44 | 0.27 | 3.36 | 0.31 | 3.38 | 0.27 |
| $\pi_{a2}\, d_{xz} \rightarrow d_{z2}\, \pi^*_{b2}$ | | 0.32 | | 0.26 | | 0.30 | | 0.31 |
| $d_{yz}\, \pi_{a2} \rightarrow d_{z2}\, \pi^*_{b1}$ | | | | | | 0.11 | | |

| | | | | | | | | |
|---|---|---|---|---|---|---|---|---|
| **$B_1$** | | | | | | | | |
| $d_{x2-y2} \rightarrow \pi^*_{b1}$ | 1.50 | 0.73 | 1.43 | 0.68 | 1.64 | 0.71 | 1.52 | 0.69 |
| $\pi_{a1} \rightarrow \pi^*_{b1}$ | 1.78 | 0.54 | 1.71 | 0.49 | 1.86 | 0.59 | 1.80 | 0.52 |
| $\pi_{a2} \rightarrow \pi^*_{b2}$ | | 0.35 | | 0.34 | | 0.23 | | 0.32 |
| $d_{x2-y2}\ \pi_{a1} \rightarrow \pi^*_{b2}\ d_{xy}$ | 2.40 | 0.61 | 2.57 | 0.56 | 2.40 | 0.54 | 2.57 | 0.61 |
| $\pi_{a1}\ d_{x2-y2} \rightarrow \pi^*_{b2}\ d_{xy}$ | | 0.20 | | 0.18 | | 0.18 | | 0.20 |
| $d_{xz} \rightarrow d_{z2}$ | 2.45 | 0.66 | 2.56 | 0.62 | 2.56 | 0.68 | 2.35 | 0.64 |
| $d_{yz} \rightarrow d_{xy}$ | | 0.19 | | 0.16 | | 0.14 | | 0.20 |
| $\pi_{a1} \rightarrow \pi^*_{b1}$ | 2.75 | 0.27 | 2.76 | 0.31 | 2.45 | 0.19 | 2.62 | 0.29 |
| $\pi_{a2} \rightarrow \pi^*_{b2}$ | | 0.43 | | 0.46 | | 0.54 | | 0.46 |
| $d_{x2-y2}\ \pi_{a2} \rightarrow \pi^*_{b1}\ d_{xy}$ | 2.77 | 0.53 | 2.94 | 0.60 | 2.76 | 0.57 | 2.86 | 0.63 |
| $\pi_{a2}\ d_{x2-y2} \rightarrow \pi^*_{b1}\ d_{xy}$ | | 0.18 | | 0.20 | | 0.19 | | 0.21 |
| $d_{x2-y2}\ \pi_{a1} \rightarrow d_{z2}\ \pi^*_{b1}$ | 3.04 | 0.58 | 3.16 | 0.55 | 3.09 | 0.57 | 3.22 | 0.59 |
| $\pi_{a1}\ d_{x2-y2} \rightarrow d_{z2}\ \pi^*_{b1}$ | | 0.19 | | 0.18 | | 0.19 | | 0.19 |
| $d_{xz} \rightarrow d_{z2}$ | 3.27 | 0.17 | 3.35 | 0.14 | 3.23 | 0.11 | 3.25 | 0.17 |
| $d_{yz} \rightarrow d_{xy}$ | | 0.62 | | 0.62 | | 0.55 | | 0.56 |

Table 7: **Active space**. Excitation energies calculated at the MS-CASPT2 level based on 10 roots for $A_1$ and $B_1$ states for various active spaces defined in the text. IPEA shift value of 0. a.u. .

Including the missing 3d' orbitals, which correlate the $3d_{z2}$ and $3d_{xy}$ orbitals, in the active space (A-CAS(14,16)), increases the excitation energies of the d→ d states of at most 0.11 eV, which is not more than the deviation observed for the other mono-excited states. The effect on the doubly excited states is larger in average, with a maximum deviation from CAS(14,14) of 0.22 eV. The effect of the $\pi^*_{CO}$ (B-CAS(14,16)) is less important on average (0.093 eV vs 0.109 eV ) with the notable exceptions of a MLCT state of $A_1$ symmetry and the second $\pi \rightarrow \pi^*$ state of $B_1$ symmetry with differences from the CAS(14,14) results of 0.23 and 0.30 eV respectively, being the largest deviations of the whole table. Although the $\pi^*_{CO}$ orbitals are not directly involved in these states, they are in the same symmetries as the $\pi^*$ orbitals of the porphyrin of the active space and influence the whole set of orbitals through their d metallic component. Note that in $B_1$ symmetry, a MLCT $d \rightarrow \pi^*_{CO}$ state is found at high energy (4.07 eV, not reported in Table 7). The addition of two $\pi^*$ orbitals of the porphyrin (C-CAS(14,16)) has limited effects on the mono-excited states (at most 0.13 eV on the second $\pi \rightarrow \pi^*$ transition) but has slightly larger effects on the doubly excited states with a maximum of 0.18 eV. To summarize, on average, CAS(14,14) results are not significantly affected by inclusion of the different couples of orbitals tested.

## Conclusion

This work presents MS-CASPT2 calculations of the singlet valence excited states of the FeP(pz)CO complex up to the Soret band (about 3.eV). The small HOMO-LUMO gap on the porphyrin ligand itself and the metal-ligand interaction induces a large diversity of excitations: d→π* transitions, d→d states, π→π* excitation of the porphyrin and some doubly excited states involving simultaneous intra-porphyrin π→π* and d→d transitions. As a consequence, the valence excited states spectrum is rather dense. Several tests on the number of roots and targeted enlargement of the active space have shown moderate effects. Omitting or including the standard IPEA shift is seen to have drastic effects on relative positions of the excited states. The importance of the effect of the IPEA is strongly correlated to the nature of the electronic excitation: d→d states are only moderately affected (<0.5 eV), while iron-to-porphyrin charge transfer states (0.5-1 eV), intra-porphyrin π→π* (about 1. eV) and doubly excited states ( ≥ 0.9 eV) are more significantly affected. As a consequence, the relative positions of d→d and π→π* states are changed when applying the standard IPEA shift. In the literature, excited states of regular porphyrins are reported to be best described without IPEA[42] while spin-state energy differences in iron compounds are reported to require higher than standard IPEA[43, 44]. Concerning our calculations on FeP(pz)CO, inclusion of the standard IPEA has a too strong effect on most of the singly excited states and it seems reasonable to either omit the shift or to reduce its value. There is a need for further investigations on the effect of IPEA on excited states of transition metal complexes. A connection between the effect of IPEA and the limitation of the active space in CASSCF/MS-CASPT2 is not to be excluded. In the present study, the active space used is rather complete for the iron but is restricted to the minimal (the Gouterman's set) for the porphyrin. Further Investigations at the RASSCF/RASPT2 level will help to clarify this point by including other orbitals of the porphyrin ring.

**Acknowledgments**

The authors thank Thomas Applencourt for technical help and acknowledge the computational resources provided by CALMIP (Toulouse).

**Supporting Information**

Coordinates of the optimized geometry (Table S1).

Excitation energies calculated at the MS-CASPT2 level based on a 10-roots SA CASSCF(14,14) without and with the inclusion of the IPEA shift of 0.25 a.u., for the $B_2$ symmetry (Table S2) and the $A_2$ symmetry (Table S3).

Additional active orbitals for the active space C-CAS(14,16) (Figure S4).

References


1. Ventalon C, Fraser JM, Vos MH, et al (2004) Coherent vibrational climbing in carboxyhemoglobin. Proc Natl Acad Sci 101:13216–13220. doi: 10.1073/pnas.0401844101

2. Treuffet J, Kubarych KJ, Lambry J-C, et al (2007) Direct observation of ligand transfer and bond formation in cytochrome c oxidase by using mid-infrared chirped-pulse upconversion. Proc Natl Acad Sci 104:15705–15710. doi: 10.1073/pnas.0703279104

3. Polack T, Ogilvie JP, Franzen S, et al (2004) CO Vibration as a Probe of Ligand Dissociation and Transfer in Myoglobin. Phys Rev Lett. doi: 10.1103/PhysRevLett.93.018102

4. Nuernberger P, Lee KF, Bonvalet A, et al (2010) Multiply Excited Vibration of Carbon Monoxide in the Primary Docking Site of Hemoglobin Following Photolysis from the Heme. J Phys Chem Lett 1:2077–2081. doi: 10.1021/jz1006324

5. Petrich JW, Poyart C, Martin JL (1988) Photophysics and reactivity of heme proteins: a femtosecond absorption study of hemoglobin, myoglobin, and protoheme. Biochemistry (Mosc) 27:4049–4060. doi: 10.1021/bi00411a022

6. Franzen S, Kiger L, Poyart C, Martin J-L (2001) Heme Photolysis Occurs by Ultrafast Excited State Metal-to-Ring Charge Transfer. Biophys J 80:2372–2385. doi: 10.1016/S0006-3495(01)76207-8

7. Dreuw A, Dunietz BD, Head-Gordon M (2002) Characterization of the Relevant Excited States in the Photodissociation of CO-Ligated Hemoglobin and Myoglobin. J Am Chem Soc 124:12070–12071. doi: 10.1021/ja026916i

8. Dunietz BD, Dreuw A, Head-Gordon M (2003) Initial Steps of the Photodissociation of the CO Ligated Heme Group. J Phys Chem B 107:5623–5629. doi: 10.1021/jp0226376

9. Ohta T, Pal B, Kitagawa T (2005) Excited State Property of Hardly Photodissociable Heme−CO Adduct Studied by Time-Dependent Density Functional Theory. J Phys Chem B 109:21110–21117. doi: 10.1021/jp052158h

10. Finley J, Malmqvist P-Å, Roos BO, Serrano-Andrés L (1998) The multi-state CASPT2 method. Chem Phys Lett 288:299–306. doi: 10.1016/S0009-2614(98)00252-8

11. Gouterman M (1959) Study of the Effects of Substitution on the Absorption Spectra of Porphin. J Chem Phys 30:1139. doi: 10.1063/1.1730148

12. Gouterman M (1961) Spectra of porphyrins. J Mol Spectrosc 6:138–163. doi: 10.1016/0022-2852(61)90236-3

13. Li Manni G, Smart SD, Alavi A (2016) Combining the Complete Active Space Self-Consistent Field Method and the Full Configuration Interaction Quantum Monte Carlo within a Super-CI Framework, with Application to Challenging Metal-Porphyrins. J Chem Theory Comput 12:1245–1258. doi: 10.1021/acs.jctc.5b01190

14. Kumar M, Pati YA, Ramasesha S (2012) A density matrix renormalization group method study of optical properties of porphines and metalloporphines. J Chem Phys 136:14112. doi: 10.1063/1.3671946

15. Perun S, Tatchen J, Marian CM (2008) Singlet and Triplet Excited States and Intersystem Crossing in Free-Base Porphyrin: TDDFT and DFT/MRCI Study. ChemPhysChem 9:282–292. doi: 10.1002/cphc.200700509

16. Aspuru-Guzik A, El Akramine O, Grossman JC, Lester WA (2004) Quantum Monte Carlo for electronic excitations of free-base porphyrin. J Chem Phys 120:3049. doi: 10.1063/1.1646356

17. Sundholm D (2000) Interpretation of the electronic absorption spectrum of free-base porphin using time-dependent density-functional theory. Phys Chem Chem Phys 2:2275–2281. doi: 10.1039/b001923m

18. Sauri V, Serrano-Andrés L, Shahi ARM, et al (2011) Multiconfigurational Second-Order Perturbation Theory Restricted Active Space (RASPT2) Method for Electronic Excited States: A Benchmark Study. J Chem Theory Comput 7:153–168. doi: 10.1021/ct100478d

19. Merchán M, Ortí E, Roos BO (1994) Theoretical determination of the electronic spectrum of free base porphin. Chem Phys Lett 226:27–36. doi: 10.1016/0009-2614(94)00681-4

20. Rubio M, Roos BO, Serrano-Andrés L, Merchán M (1999) Theoretical study of the electronic spectrum of magnesium-porphyrin. J Chem Phys 110:7202. doi: 10.1063/1.478624

21. Serrano-Andrés L, Merchán M, Rubio M, Roos BO (1998) Interpretation of the electronic absorption spectrum of free base porphin by using multiconfigurational

second-order perturbation theory. Chem Phys Lett 295:195–203. doi: 10.1016/S0009-2614(98)00934-8

22. Fransson T, Saue T, Norman P (2016) Four-Component Damped Density Functional Response Theory Study of UV/Vis Absorption Spectra and Phosphorescence Parameters of Group 12 Metal-Substituted Porphyrins. J Chem Theory Comput 12:2324–2334. doi: 10.1021/acs.jctc.6b00030

23. Chen H, Lai W, Shaik S (2011) Multireference and Multiconfiguration Ab Initio Methods in Heme-Related Systems: What Have We Learned So Far? J Phys Chem B 115:1727–1742. doi: 10.1021/jp110016u

24. Vancoillie S, Zhao H, Radoń M, Pierloot K (2010) Performance of CASPT2 and DFT for Relative Spin-State Energetics of Heme Models. J Chem Theory Comput 6:576–582. doi: 10.1021/ct900567c

25. Radoń M, Broclawik E, Pierloot K (2010) Electronic Structure of Selected $\{FeNO\}^7$ Complexes in Heme and Non-Heme Architectures: A Density Functional and Multireference ab Initio Study. J Phys Chem B 114:1518–1528. doi: 10.1021/jp910220r

26. Radoń M, Pierloot K (2008) Binding of CO, NO, and $O_2$ to Heme by Density Functional and Multireference ab Initio Calculations. J Phys Chem A 112:11824–11832. doi: 10.1021/jp806075b

27. Ribas-Ariño J, Novoa JJ (2007) The mechanism for the reversible oxygen addition to heme. A theoretical CASPT2 study. Chem Commun 3160. doi: 10.1039/b704871h

28. Kitagawa Y, Chen Y, Nakatani N, et al (2016) A DFT and Multi-Configurational Perturbation Theory Study on $O_2$ Binding to a Model Heme Compound Via the Spin-Change Barrier. Phys Chem Chem Phys 18:18137–18144. doi: 10.1039/C6CP02329K

29. Jensen K, Roos B, Ryde U (2005) O-binding to heme: electronic structure and spectrum of oxyheme, studied by multiconfigurational methods. J Inorg Biochem 99:45–54. doi: 10.1016/j.jinorgbio.2004.11.008

30. Chen H, Ikeda-Saito M, Shaik S (2008) Nature of the Fe−$O_2$ Bonding in Oxy-Myoglobin: Effect of the Protein. J Am Chem Soc 130:14778–14790. doi: 10.1021/ja805434m

31. Kepenekian M, Calborean A, Vetere V, et al (2011) Toward Reliable DFT Investigations of Mn-Porphyrins through CASPT2/DFT Comparison. J Chem Theory Comput 7:3532–3539. doi: 10.1021/ct2004066

32. Alcover-Fortuny G, Caballol R, Pierloot K, de Graaf C (2016) Role of the Imide Axial Ligand in the Spin and Oxidation State of Manganese Corrole and Corrolazine Complexes. Inorg Chem 55:5274–5280. doi: 10.1021/acs.inorgchem.6b00194

33. Roos BO, Taylor PR, Per E.M. Siegbahn (1980) A complete active space SCF method (CASSCF) using a density matrix formulated super-CI approach. Chem Phys 48:157–173. doi: 10.1016/0301-0104(80)80045-0

34. Malmqvist PÅ, Pierloot K, Shahi ARM, et al (2008) The restricted active space followed by second-order perturbation theory method: Theory and application to the study of $CuO_2$ and $Cu_2O_2$ systems. J Chem Phys 128:204109. doi: 10.1063/1.2920188

35. Vancoillie S, Zhao H, Tran VT, et al (2011) Multiconfigurational Second-Order Perturbation Theory Restricted Active Space (RASPT2) Studies on Mononuclear First-Row Transition-Metal Systems. J Chem Theory Comput 7:3961–3977. doi: 10.1021/ct200597h

36. Venturinelli Jannuzzi SA, Phung QM, Domingo A, et al (2016) Spin State Energetics and Oxyl Character of Mn-Oxo Porphyrins by Multiconfigurational ab Initio Calculations: Implications on Reactivity. Inorg Chem 55:5168–5179. doi: 10.1021/acs.inorgchem.5b02920

37. Radoń M, Broclawik E, Pierloot K (2011) DFT and Ab Initio Study of Iron-Oxo Porphyrins: May They Have a Low-Lying Iron(V)-Oxo Electromer? J Chem Theory Comput 7:898–908. doi: 10.1021/ct1006168

38. Zhao H, Pierloot K, Langner EHG, et al (2012) Low-Energy States of Manganese–Oxo Corrole and Corrolazine: Multiconfiguration Reference ab Initio Calculations. Inorg Chem 51:4002–4006. doi: 10.1021/ic201972f

39. Nakatsuji H, Tokita Y, Hasegawa J, Hada M (1996) Ground and excited states of carboxyheme: a SAC/SAC-CI study. Chem Phys Lett 256:220–228. doi: 10.1016/0009-2614(96)00386-7

40. Tokita Y, Nakatsuji H (1997) Ground and Excited States of Hemoglobin CO and Horseradish Peroxidase CO: SAC/SAC-CI Study. J Phys Chem B 101:3281–3289. doi: 10.1021/jp963805v

41. Ghigo G, Roos BO, Malmqvist P-Å (2004) A modified definition of the zeroth-order Hamiltonian in multiconfigurational perturbation theory (CASPT2). Chem Phys Lett 396:142–149. doi: 10.1016/j.cplett.2004.08.032

42. Kerridge A (2013) A RASSCF study of free base, magnesium and zinc porphyrins: accuracy versus efficiency. Phys Chem Chem Phys 15:2197–2209. doi: 10.1039/C2CP43982D

43. Vela S, Fumanal M, Ribas-Ariño J, Robert V (2016) On the zeroth-order hamiltonian for CASPT2 calculations of spin crossover compounds: Spin State Energetics of $FeN_6^-$ Based SCO Compounds. J Comput Chem 37:947–953. doi: 10.1002/jcc.24283

44. Kepenekian M, Robert V, Le Guennic B (2009) What zeroth-order Hamiltonian for CASPT2 adiabatic energetics of Fe(II)$N_6$ architectures? J Chem Phys 131:114702. doi: 10.1063/1.3211020

45. Radoń M, Rejmak P, Fitta M, et al (2015) How can $[Mo^{IV}(CN)_6]^{2-}$, an apparently octahedral $(d)^2$ complex, be diamagnetic? Insights from quantum chemical calculations and magnetic susceptibility measurements. Phys Chem Chem Phys 17:14890–14902. doi: 10.1039/C4CP04863F

46. Ruipérez F, Aquilante F, Ugalde JM, Infante I (2011) Complete vs Restricted Active Space Perturbation Theory Calculation of the $Cr_2$ Potential Energy Surface. J Chem Theory Comput 7:1640–1646. doi: 10.1021/ct200048z

47. Adamo C, Barone V (1999) Toward reliable density functional methods without adjustable parameters: The PBE0 model. J Chem Phys 110:6158. doi: 10.1063/1.478522

48. Weigend F, Ahlrichs R (2005) Balanced basis sets of split valence, triple zeta valence and quadruple zeta valence quality for H to Rn: Design and assessment of accuracy. Phys Chem Chem Phys 7:3297. doi: 10.1039/b508541a

49. Weigend F (2006) Accurate Coulomb-fitting basis sets for H to Rn. Phys Chem Chem Phys 8:1057. doi: 10.1039/b515623h

50. Frisch, M. J.; Trucks, G. W.; Schlegel, H. B.; Scuseria, G. E.; Robb, M. A.; Cheeseman, J. R.; Scalmani, G.; Barone, V.; Mennucci, B.; Petersson, G. A.; Nakatsuji, H.; Caricato, M.; Li, X.; Hratchian, H. P.; Izmaylov, A. F.; Bloino, J.; Zheng, G.; Sonnenberg, J. L.; Hada, M.; Ehara, M.; Toyota, K.; Fukuda, R.; Hasegawa, J.; Ishida, M.; Nakajima, T.; Honda, Y.; Kitao, O.; Nakai, H.; Vreven, T.; Montgomery, J. A., Jr.; Peralta, J. E.; Ogliaro, F.; Bearpark, M.; Heyd, J. J.; Brothers, E.; Kudin, K. N.; Staroverov, V. N.; Kobayashi, R.; Normand, J.; Raghavachari, K.; Rendell, A.; Burant, J. C.; Iyengar, S. S.; Tomasi, J.; Cossi, M.; Rega, N.; Millam, J. M.; Klene, M.; Knox, J. E.; Cross, J. B.; Bakken, V.; Adamo, C.; Jaramillo, J.; Gomperts, R.; Stratmann, R. E.; Yazyev, O.; Austin, A. J.; Cammi, R.; Pomelli, C.; Ochterski, J. W.; Martin, R. L.; Morokuma, K.; Zakrzewski, V. G.; Voth, G. A.; Salvador, P.; Dannenberg, J. J.; Dapprich, S.; Daniels, A. D.; Farkas, Ö.; Foresman, J. B.; Ortiz, J. V.; Cioslowski, J.; Fox, D. J. (2009) Gaussian 09. Gaussian, Inc., Wallingford CT,

51. Bode BM, Gordon MS (1998) Macmolplt: a graphical user interface for GAMESS. J Mol Graph Model 16:133–138. doi: 10.1016/S1093-3263(99)00002-9

52. Aquilante F, De Vico L, Ferré N, et al (2010) MOLCAS 7: The Next Generation. J Comput Chem 31:224–247. doi: 10.1002/jcc.21318

53. Karlström G, Lindh R, Malmqvist P-Å, et al (2003) MOLCAS: a program package for computational chemistry. Comput Mater Sci 28:222–239. doi: 10.1016/S0927-0256(03)00109-5

54. Veryazov V, Widmark P-O, Serrano-Andrés L, et al (2004) MOLCAS as a development platform for quantum chemistry software: MOLCAS: Software Development Platform. Int J Quantum Chem 100:626–635. doi: 10.1002/qua.20166

55. Roos BO, Lindh R, Malmqvist P-Å, et al (2004) Main Group Atoms and Dimers Studied with a New Relativistic ANO Basis Set. J Phys Chem A 108:2851–2858. doi: 10.1021/jp031064+

56. Roos BO, Lindh R, Malmqvist P-Å, et al (2005) New Relativistic ANO Basis Sets for Transition Metal Atoms. J Phys Chem A 109:6575–6579. doi: 10.1021/jp0581126

57. Douglas M, Kroll NM (1974) Quantum electrodynamical corrections to the fine structure of helium. Ann Phys 82:89–155. doi: 10.1016/0003-4916(74)90333-9

58. Jansen G, Hess BA (1989) Revision of the Douglas-Kroll transformation. Phys Rev A 39:6017. doi: 10.1103/PhysRevA.39.6016

59. Balabanov NB, Peterson KA (2005) Systematically convergent basis sets for transition metals. I. All-electron correlation consistent basis sets for the 3d elements Sc–Zn. J Chem Phys 123:64107. doi: 10.1063/1.1998907

60. Varetto U, Molekel 5.4.

61. Aquilante F, Pedersen TB, Lindh R (2007) Low-cost evaluation of the exchange Fock matrix from Cholesky and density fitting representations of the electron repulsion integrals. J Chem Phys 126:194106. doi: 10.1063/1.2736701

62. Aquilante F, Malmqvist P-Å, Pedersen TB, et al (2008) Cholesky Decomposition-Based Multiconfiguration Second-Order Perturbation Theory (CD-CASPT2): Application to the Spin-State Energetics of $Co^{III}$(diiminato)(NPh). J Chem Theory Comput 4:694–702. doi: 10.1021/ct700263h

63. Andersson K (1995) Different forms of the zeroth-order Hamiltonian in second-order perturbation theory with a complete active space self-consistent field reference function. Theor Chim Acta 91:31–46. doi: 10.1007/BF01113860

64. Makinen MW, Eaton WA (1973) Polarized single crystal absorption spectra of carboxy- and oxyhemoglobin. Ann N Y Acad Sci 206:210–222. doi: 10.1111/j.1749-6632.1973.tb43213.x

# Supplementary Information about

# "Valence excited states of metalloporphyrins studied with the CASPT2 method: the case of an Iron complex"

*Nadia Ben Amor*, Adrien Soupart, Marie-Catherine Heitz**

| | | | |
|---|---|---|---|
| Fe | 0.000000 | 0.000000 | -0.044953 |
| C | 0.000000 | 0.000000 | 1.738656 |
| C | 2.767584 | 1.229204 | 0.007914 |
| C | -2.767584 | 1.229204 | 0.007914 |
| C | 2.767584 | -1.229204 | 0.007914 |
| C | -2.767584 | -1.229204 | 0.007914 |
| C | 1.229179 | 2.761585 | -0.134930 |
| C | -1.229179 | 2.761585 | -0.134930 |
| C | 1.229179 | -2.761585 | -0.134930 |
| C | -1.229179 | -2.761585 | -0.134930 |
| C | 2.491938 | 3.447272 | -0.101547 |
| C | -2.491938 | 3.447272 | -0.101547 |
| C | 2.491938 | -3.447272 | -0.101547 |
| C | -2.491938 | -3.447272 | -0.101547 |
| C | 3.448090 | 2.495181 | -0.004897 |
| C | -3.448090 | 2.495181 | -0.004897 |
| C | 3.448090 | -2.495181 | -0.004897 |
| C | -3.448090 | -2.495181 | -0.004897 |
| C | 0.000000 | 3.394071 | -0.180465 |
| C | 0.000000 | -3.394071 | -0.180465 |
| C | 3.401747 | 0.000000 | 0.064482 |
| C | -3.401747 | 0.000000 | 0.064482 |
| C | 1.133575 | 0.000000 | -2.823100 |
| C | -1.133575 | 0.000000 | -2.823100 |
| C | 1.123867 | 0.000000 | -4.208894 |
| C | -1.123867 | 0.000000 | -4.208894 |
| O | 0.000000 | 0.000000 | 2.873911 |
| N | 0.000000 | 0.000000 | -2.124772 |
| N | 0.000000 | 0.000000 | -4.912649 |
| N | 1.421423 | 1.415583 | -0.077949 |
| N | -1.421423 | 1.415583 | -0.077949 |
| N | 1.421423 | -1.415583 | -0.077949 |
| N | -1.421423 | -1.415583 | -0.077949 |
| H | 4.483096 | 0.000000 | 0.132927 |
| H | -4.483096 | 0.000000 | 0.132927 |
| H | 0.000000 | 4.476824 | -0.220913 |
| H | 0.000000 | -4.476824 | -0.220913 |

| | | | |
|---|---|---|---|
| H | 2.059971 | 0.000000 | -2.264572 |
| H | -2.059971 | 0.000000 | -2.264572 |
| H | 2.058639 | 0.000000 | -4.760403 |
| H | -2.058639 | 0.000000 | -4.760403 |
| H | 2.612054 | 4.520112 | -0.139158 |
| H | -2.612054 | 4.520112 | -0.139158 |
| H | 2.612054 | -4.520112 | -0.139158 |
| H | -2.612054 | -4.520112 | -0.139158 |
| H | 4.519599 | 2.620206 | 0.050942 |
| H | -4.519599 | 2.620206 | 0.050942 |
| H | 4.519599 | -2.620206 | 0.050942 |
| H | -4.519599 | -2.620206 | 0.050942 |

Table S1: **Coordinates of the Optimized structure (in Angströms)**

| **$B_2$** | | **No IPEA** | | | **Standard IPEA (0.25 a.u.)** |
|---|---|---|---|---|---|
| State | ΔE (eV) | Weight | | ΔE (eV) | Weight |
| $d_{x2-y2}$ -> $\pi^*_{b2}$ | 1.52 | 0.73 | $d_{x2-y2}$ -> $\pi^*_{b2}$ | 2.01 | 0.73 |
| $\pi_{a2}$ -> $\pi^*_{b1}$ | 1.80 | 0.37 | $d_{yz}$ -> $d_{z2}$ | 2.67 | 0.65 |
| $\pi_{a1}$ -> $\pi^*_{b2}$ | | 0.52 | $d_{xz}$ -> $d_{xy}$ | | 0.21 |
| $d_{x2-y2}$ $\pi_{a1}$ -> $\pi^*_{b1}$ $d_{xy}$ | 2.38 | 0.61 | $\pi_{a2}$ -> $\pi^*_{b1}$ | 2.76 | 0.40 |
| $\pi_{a1}$ $d_{x2-y2}$ -> $\pi^*_{b1}$ $d_{xy}$ | | 0.20 | $\pi_{a1}$ -> $\pi^*_{b2}$ | | 0.48 |
| $d_{yz}$ -> $d_{z2}$ | 2.45 | 0.67 | $d_{x2-y2}$ $\pi_{a1}$ -> $\pi^*_{b1}$ $d_{xy}$ | 3.34 | 0.63 |
| $d_{xz}$ -> $d_{xy}$ | | 0.19 | $\pi_{a1}$ $d_{x2-y2}$ -> $\pi^*_{b1}$ $d_{xy}$ | | 0.21 |
| $\pi_{a2}$ -> $\pi^*_{b1}$ | 2.79 | 0.35 | $d_{yz}$ -> $d_{z2}$ | 3.58 | 0.18 |
| $\pi_{a1}$ -> $\pi^*_{b2}$ | | 0.25 | $d_{xz}$ -> $d_{xy}$ | | 0.60 |
| $d_{x2-y2}$ $\pi_{a2}$ -> $\pi^*_{b2}$ $d_{xy}$ | | 0.15 | | | |
| $d_{x2-y2}$ $\pi_{a2}$ -> $\pi^*_{b2}$ $d_{xy}$ | 2.80 | 0.46 | $d_{x2-y2}$ $\pi_{a2}$ -> $\pi^*_{b2}$ $d_{xy}$ | 3.68 | 0.63 |
| $\pi_{a2}$ $d_{x2-y2}$ -> $\pi^*_{b2}$ $d_{xy}$ | | 0.15 | $\pi_{a2}$ $d_{x2-y2}$ -> $\pi^*_{b2}$ $d_{xy}$ | | 0.21 |
| $\pi_{a1}$ -> $\pi^*_{b2}$ | | 0.12 | $\pi_{a1}$ -> $\pi^*_{b2}$ | | < 0.01 |
| $d_{x2-y2}$ $\pi_{a1}$ -> $d_{z2}$ $\pi^*_{b2}$ | 3.07 | 0.57 | $\pi_{a2}$ -> $\pi^*_{b1}$ | 3.90 | 0.44 |
| $\pi_{a1}$ $d_{x2-y2}$ -> $d_{z2}$ $\pi^*_{b2}$ | | 0.18 | $\pi_{a1}$ -> $\pi^*_{b2}$ | | 0.36 |
| | | | $d_{x2-y2}$ $\pi_{a2}$ -> $\pi^*_{b2}$ $d_{xy}$ | | <0.01 |
| $d_{yz}$ -> $d_{z2}$ | 3.29 | 0.17 | $d_{x2-y2}$ $\pi_{a1}$ -> $d_{z2}$ $\pi^*_{b2}$ | 4.02 | 0.60 |
| $d_{xz}$ -> $d_{xy}$ | | 0.62 | $\pi_{a1}$ $d_{x2-y2}$ -> $d_{z2}$ $\pi^*_{b2}$ | | 0.19 |

Table S2: **IPEA shift**. Excitation energies calculated at the MS-CASPT2 level based on a 10-roots SA CASSCF(14,14) without and with the inclusion of the IPEA shift of 0.25 a.u. (standard value), for the $B_2$ symmetry.

| $A_2$ | No IPEA | | Standard IPEA (0.25 a.u.) | | |
|---|---|---|---|---|---|
| State | ΔE (eV) | Weight | | ΔE (eV) | Weight |
| $d_{yz}$ -> $\pi^*_{b1}$ | 1.86 | 0.14 | $d_{x2-y2}$ -> $d_{xy}$ | 2.16 | 0.83 |
| $d_{xz}$ -> $\pi^*_{b2}$ | | 0.54 | | | |
| $d_{yz}$ -> $\pi^*_{b1}$ | 1.89 | 0.56 | $d_{yz}$ -> $\pi^*_{b1}$ | 2.38 | 0.71 |
| $d_{xz}$ -> $\pi^*_{b2}$ | | 0.13 | $d_{xz}$ -> $\pi^*_{b2}$ | | 0.02 |
| $d_{x2-y2}$ -> $d_{xy}$ | 2.05 | 0.76 | $d_{yz}$ -> $\pi^*_{b1}$ | 2.40 | 0.02 |
| | | | $d_{xz}$ -> $\pi^*_{b2}$ | | 0.71 |
| $\pi_{a1}$ -> $d_{xy}$ | 2.23 | 0.25 | $\pi_{a2}$ -> $d_{z2}$ | 3.47 | 0.25 |
| $d_{yz}$ $\pi_{a1}$ -> $\pi^*_{b2}$ $d_{xy}$ | | 0.18 | $\pi_{a2}$ $d_{yz}$ -> $d_{z2}$ $\pi^*_{b2}$ | | 0.30 |
| $d_{xz}$ $\pi_{a1}$ -> $\pi^*_{b1}$ $d_{xy}$ | | 0.16 | $\pi_{a2}$ $d_{xz}$ -> $d_{z2}$ $\pi^*_{b1}$ | | 0.30 |
| $\pi_{a2}$ -> $d_{z2}$ | 2.55 | 0.24 | $\pi_{a1}$ -> $d_{xy}$ | 3.52 | 0.29 |
| $\pi_{a2}$ $d_{yz}$ -> $d_{z2}$ $\pi^*_{b2}$ | | 0.29 | $d_{yz}$ $\pi_{a1}$ -> $\pi^*_{b2}$ $d_{xy}$ | | 0.20 |
| $\pi_{a2}$ $d_{xz}$ -> $d_{z2}$ $\pi^*_{b1}$ | | 0.27 | $d_{xz}$ $\pi_{a1}$ -> $\pi^*_{b1}$ $d_{xy}$ | | 0.19 |
| $d_{yz}$ $\pi_{a1}$ -> $\pi^*_{b1}$ $d_{z2}$ | 2.97 | 0.26 | $d_{yz}$ $\pi_{a1}$ -> $\pi^*_{b1}$ $d_{z2}$ | 4.40 | 0.16 |
| $d_{yz}$ $\pi_{a1}$ -> $d_{z2}$ $\pi^*_{b1}$ | | 0.09 | $d_{yz}$ $\pi_{a1}$ -> $d_{z2}$ $\pi^*_{b1}$ | | 0.06 |
| $\pi_{a1}$ $d_{xz}$ -> $d_{z2}$ $\pi^*_{b2}$ | | 0.17 | $\pi_{a1}$ $d_{xz}$ -> $d_{z2}$ $\pi^*_{b2}$ | | 0.27 |
| $d_{yz}$ $\pi_{a1}$ -> $\pi^*_{b1}$ $d_{z2}$ | 3.02 | 0.22 | $d_{yz}$ $\pi_{a1}$ -> $\pi^*_{b1}$ $d_{z2}$ | 4.44 | 0.35 |
| $d_{yz}$ $\pi_{a1}$ -> $d_{z2}$ $\pi^*_{b1}$ | | 0.09 | $d_{yz}$ $\pi_{a1}$ -> $d_{z2}$ $\pi^*_{b1}$ | | 0.14 |
| $\pi_{a1}$ $d_{xz}$ -> $d_{z2}$ $\pi^*_{b2}$ | | 0.30 | $\pi_{a1}$ $d_{xz}$ -> $d_{z2}$ $\pi^*_{b2}$ | | 0.24 |
| $d_{xz}$ $\pi_{a1}$ -> $d_{z2}$ $\pi^*_{b2}$ | | 0.12 | $d_{xz}$ $\pi_{a1}$ -> $d_{z2}$ $\pi^*_{b2}$ | | 0.10 |
| $d_{yz}$ $\pi_{a2}$ -> $\pi^*_{b1}$ $d_{xy}$ | 3.27 | 0.13 | $d_{yz}$ $\pi_{a2}$ -> $\pi^*_{b1}$ $d_{xy}$ | 4.55 | 0.14 |
| $\pi_{a2}$ $d_{yz}$ -> $d_{z2}$ $\pi^*_{b2}$ | | 0.24 | $\pi_{a2}$ $d_{yz}$ -> $d_{z2}$ $\pi^*_{b2}$ | | 0.31 |
| $\pi_{a2}$ $d_{xz}$ -> $d_{z2}$ $\pi_{b1}$* | | 0.27 | $\pi_{a2}$ $d_{xz}$ -> $d_{z2}$ $\pi_{b1}$* | | 0.31 |

Table S3: **IPEA shift**. Excitation energies calculated at the MS-CASPT2 level based on a 10-roots SA CASSCF(14,14) without and with the inclusion of the IPEA shift of 0.25 a.u. (standard value), for the $A_2$ symmetry.


Figure S4: **Additional active orbitals** for the active space C-CAS(14,16)